Enhancing Wear Resistance of EN-19 Steel with Physical Vapor Deposition (PVD) Coatings: Experimental and Statistical Analysis

Arshpreet Kaur
Department of Mechanical Engineering, Punjabi University

Jasminder Singh Dureja
Department of Mechanical Engineering, Punjabi University

Jasmaninder Singh Grewal
Department of Mechanical & Production Engineering, Guru Nanak Dev Engineering College

https://doi.org/10.5109/7420066

出版情報：Evergreen. 13 (2), pp.517-536, 2026-06. 九州大学グリーンテクノロジー研究教育センター
バージョン：

Enhancing Wear Resistance of EN-19 Steel with Physical Vapor Deposition (PVD) Coatings: Experimental and Statistical Analysis

Arshpreet Kaur[1,*], Jasminder Singh Dureja[1], Jasmaninder Singh Grewal[2]

[1]Department of Mechanical Engineering, Punjabi University, Patiala, India
[2]Department of Mechanical and Production Engineering, Guru Nanak Dev Engineering College, Ludhiana, 141006, Punjab, India

*Author to whom correspondence should be addressed:
E-mail: arshpandher89@gmail.com

(Received September 13, 2025; Revised November 29, 2025; Accepted March 24, 2026)

Abstract: To increase the durability of automobile components, this study investigates the wear behavior of EN-19 steel under various tribological environments, both with and without protective coatings. Physical vapor deposition (PVD) was used to produce the AlTiN and AlCrN coatings, which were then tested utilizing ball-on-disc studies at various loads, sliding velocities, and time durations. According to the results, AlCrN performed best, with coated specimens showing a considerable decrease in wear loss, while uncoated samples suffered the most wear. Coating type and time were found to be the primary determinants of wear, as determined by statistical analysis using the Box-Cox transformation, whereas load and velocity had secondary effects. Using contour and residual plots, regression modeling ($\lambda = 0.7$) produced accurate predictions. Compared with uncoated steel, AlCrN reduced overall wear by up to 55%, demonstrating its suitability for applications such as CV joints. The results demonstrate the significance of specific coatings in enhancing wear resistance and prolonging the useful life of engineering components.

Keywords: EN-19 Steel; Predictive Modeling; PVD Coatings; Tribological Performance; Wear Behavior

1. Introduction

Modern manufacturing and automotive applications demand advanced materials with enhanced wear resistance, thermal stability, and extended service life. Components such as bearings, cutting tools, and constant-velocity (CV) joints often operate in challenging tribological environments, where wear and friction can significantly affect performance and efficiency. Protective coatings like aluminum chromium nitride (AlCrN, commercially known as Alcrona) and aluminum titanium nitride (AlTiN, commercially known as Latuma) deposited via physical vapor deposition (PVD) have emerged as promising solutions to address these issues due to their high hardness, oxidation resistance, and tribological behavior[1,2)].

Recent research indicates that alloying elements, coating architecture, and deposition techniques significantly impact the performance of these coatings. Hardness and oxidation resistance were enhanced by the inclusion of Si or Ni, which enhanced machining performance in demanding settings[3,4)]. On the other hand, compared to uncoated tools, nano multilayer AlTiN/TiN systems demonstrated superior wear resistance and longer tool life[5)]. Similarly, AlCrN-based coatings alloyed with Mo and Nb showed superior wear resistance during the machining of Inconel 718[6)].

This study investigates the wear behavior of AlCrN and AlTiN coatings on EN-19 steel under varied loads, speeds, time durations, and ambient conditions to optimize performance for industrial applications.

1.1. Problem Formulation

EN-19 steel, used in CV joints, gears, and shafts, is prone to adhesive and abrasive wear due to high stresses, elevated temperatures, and dry sliding, reducing reliability and service life. Conventional methods such as lubrication and alloying offer only partial improvement. Advanced PVD coatings such as AlCrN and AlTiN offer hardness, oxidation resistance, and tribological stability, but their comparative performance on EN-19 under varying loads, velocities, and durations remains underexplored. Moreover, predictive statistical modeling to guide coating selection is lacking. This study addresses these gaps by experimentally evaluating and statistically analyzing the wear behavior of coated and uncoated EN-19 steel for

Cite: A. Kaur, J. Dureja, J. Grewal, "Enhancing Wear Resistance of EN-19 Steel with Physical Vapor Deposition (PVD) Coatings: Experimental and Statistical Analysis". Evergreen, 13 (02) 517-536 (2026). https://doi.org/10.5109/7420066.

automotive applications.

Although extensive research has been conducted on nitride-based PVD coatings such as AlTiN, TiAlN, and AlCrN, most published work focuses on tool steels or machining conditions at high sliding speeds and in room-temperature environments. For example, Claudin[7] demonstrated that AlCrN and TiAlN coatings provide superior friction performance during high-speed dry machining of AISI 4140 steel. Still, the study did not consider sustained thermal exposure or automotive drivetrain conditions. Similarly, Rech[8] and Podgornik[9] evaluated PVD-coated AISI 4140 steel under dry sliding. Yet, their investigations were limited to machining regimes and plasma-nitrided substrates rather than automotive-grade steels under thermal loading. These existing studies highlight coating superiority but offer neither a predictive modelling framework nor analysis at moderate-to-high temperatures relevant to CV-joint operation.

More recent Evergreen and tribology contributions reinforce this research gap. Burshukova[10] explored nanostructured damping alloys for noise–vibration reduction in vehicles, while Dubey[11] investigated hard chrome coatings under room-temperature dry sliding. Likewise, Grover[12] analyzed atmospheric corrosion of zinc coatings for structural durability. Mohd-Azmi[13] evaluated the thermal resistance of intumescent coatings. While valuable, these works do not address the wear mechanisms of AlTiN/AlCrN on EN-19 (AISI 4140-equivalent) steel, nor the influence of coatings under continuous sliding at elevated temperatures such as 200 °C, which is typical for CV-joint housings and drivetrain components.

Furthermore, advanced coating technologies for harsh environments (e.g., marine tribocorrosion) have been documented[14]. Kumar[15] have also been reported multilayer ceramic coatings for erosion . However, these studies focus on corrosion–wear or particle erosion, not on automotive steel sliding wear, and none incorporate a Box–Cox transformation-based regression model to predict wear behaviour. To the authors' knowledge, no published study combines experimental dry sliding tests of AlCrN/AlTiN on EN-19 steel at 200 °C with statistical modelling capable of capturing coating-specific effects.

This study is novel because:

It is among the first to evaluate the dry sliding wear behaviour of AlTiN and AlCrN coatings on EN-19 steel at 200 °C, a temperature regime directly relevant to CV-joint and drivetrain operating conditions but rarely examined in prior tribology literature.

It develops a Box–Cox–based predictive regression model that explicitly incorporates coating type as a statistical factor, enabling more accurate wear-life estimation of coated automotive steels than conventional ANOVA-only approaches reported in earlier studies.

It offers a combined experimental and statistical framework that supports durability design for automotive drivetrain components, advancing beyond existing work that focuses solely on friction measurements or machining environments.

The automotive sector is increasingly transitioning toward sustainability-driven manufacturing, aligned with the Green Asia vision that emphasizes energy efficiency, resource conservation, and reduced environmental burden. CV joints are widely used in modern vehicles, and their failure or excessive wear can lead to frequent replacements, increased maintenance costs, and increased demand for raw materials. The implementation of advanced protective coatings, such as AlCrN and AlTiN, can significantly reduce wear and friction, extending the service life of drivetrain components. The results are directly aligned and contribute to reduced steel consumption, lower energy consumption in production, and minimized disposal of worn components. Enhanced wear resistance supports lightweight drivetrain designs by enabling reduced component over-dimensioning. Thereby improving fuel economy and lowering CO_2 emissions. The tribological improvements demonstrated in this work reinforce the role of surface coatings in accelerating the shift toward economical and greener automotive systems across emerging Asian markets.

1.2. Research Objectives

The current study is being conducted with the following research objectives:

A ball-on-disc tribometer will be used to examine the wear behavior of EN-19 steel under uncoated, AlTiN, and AlCrN (AlCrN) coated conditions under various loads, sliding velocities, and test durations.

To determine the primary factors influencing wear performance and examine the impact of tribological parameters (load, velocity, and time) on wear loss.

- To compare the effectiveness of AlCrN and AlTiN coatings in increasing the wear resistance of EN-19 steel to assess their suitability for automotive applications, such as CV joints.
- To use statistical methods for accurate wear behavior prediction and optimization, such as regression modeling and Box-Cox transformation.
- To offer a scientific foundation for choosing suitable PVD coatings to increase the lifespan of EN-19 steel parts subjected to harsh tribological conditions.

1.3. Importance of the Study

This work addresses the persistent wear problem in EN-19 steel, widely used in automotive shafts, gears, and CV joints operating under harsh tribological conditions. By applying advanced PVD coatings (AlTiN and AlCrN), the study demonstrates improved wear resistance, reduced

Cite: A. Kaur, J. Dureja, J. Grewal, "Enhancing Wear Resistance of EN-19 Steel with Physical Vapor Deposition (PVD) Coatings: Experimental and Statistical Analysis". Evergreen, 13 (02) 517-536 (2026). https://doi.org/10.5109/7420066.

material loss, and extended component life at high loads, speeds, time, and ambient conditions. A prediction framework for maximizing coating performance and operating conditions is provided by the combination of statistical modeling and Box-Cox transformation. In addition to supporting robust and energy-efficient automotive systems, these findings improve tribology and close the gap between predictive modeling and realistic surface engineering for dependable industrial applications.

1.4. Literature Review

Advanced protective coatings such as AlCrN and AlTiN are in high demand for their exceptional wear resistance and suitability for challenging tribological conditions. It has been demonstrated that improving coating structures with multilayers and bias control techniques increases hardness and fracture toughness, prolonging tool life during dry machining[16,17].Nitriding and other substrate pre-treatment techniques increase adhesion and load-bearing capability, which in turn improves AlCrN and related coating resistance to high-temperature wear[18]. Further evidence of superior performance over monolayer coatings under extreme cutting circumstances comes from comparative investigations on bilayer topologies, such as AlTiN/TiAlSiN[19].

According to dynamic-mechanical research, microstructural changes, such as CrN precipitation in AlCrN films, might advantageously enhance damping characteristics and modulus, offering fresh perspectives on thermal stability and performance[20]. Through the modification of advanced microgeometry, nano-multilayer TiN/AlTiN coatings greatly increase endurance in tool applications[21,22]. Furthermore, by creating lubricating tribolayers, tribochemical techniques such as AlTiN/a-C nanocomposites reduce friction and improve wear resistance[23]. Recent developments in BP-HPPMS-fabricated bilayer AlTiN/TiSiN coatings show their applicability for high-performance tribological applications by exhibiting variable hardness and wear resistance[24]. These studies collectively demonstrate the critical importance of innovative designs, substrate treatment, and structural design in improving coating performance, consistent with the current study's emphasis on enhancing wear resistance.

Recent developments in hard coatings, such as AlCrN and AlTiN, have shown notable gains in machinability, wear resistance, and friction reduction under challenging operating circumstances. Optimal AlTiN bilayer coatings offer longer tool life than monolayers in high-speed machining of stainless steels, whereas variations in Al/Ti ratios and multilayer structures impact mechanical and tribological performance[25,26]. Similarly, at high pressures and temperatures, adhesion is improved, and tribological behavior is enhanced by substrate engineering and interlayer alterations, such as the addition of AlCrN or TiN[27]. Comparative studies confirm that AlTiSiN coatings, especially those produced by scalable pulsed power plasma, outperform conventional AlTiN by reducing flank wear and extending tool life in hard turning of tool steels[28]. Novel alloying approaches also improve coating performance. For instance, AlCrN/Cu hybrid coatings reduce friction at high temperatures due to the formation of oxide phases, while multilayer TiAlCrSiN/TiAlCrN coatings generate self-organized tribo-films, enhancing tool life during machining of Inconel alloys[29,30]. Taguchi-based optimization studies further establish the effectiveness of coated inserts in reducing surface roughness and wear in aluminum and steel machining[31]. Additionally, micro-milling studies show that AlTiN-coated WC tools combined with nano-MQL significantly improve the machinability of Ti6Al4V alloys[32]. Collectively, these findings highlight the importance of coating composition, architecture, and lubrication strategies in enhancing wear resistance, directly supporting the present study's emphasis on coating performance for tribological applications.

Advances in nitride-based coatings, especially AlTiN and AlCrN, have drawn attention because of their better hardness, wear resistance, and stability at high temperatures. Numerous studies have shown how alloying elements, coating design, and deposition techniques can improve tool life and tribological performance. For example, AlTiN coatings mechanical toughness and wear resistance were increased via hybrid deposition techniques that included arc evaporation and magnetron sputtering, which decreased residual stress and increased thermal stability[33]. Similarly, multilayer and nanocomposite strategies, such as AlCrSiN–Ni/AlCrN, improved hardness and scratch toughness, significantly lowering wear rates at elevated temperatures[34].

Oxidation, adhesion, and fatigue are the main wear mechanisms in coated tools; research has shown that AlTiBN, AlTiTaN, and AlTiN hybrid coatings are more resistant to harsh circumstances[35,36]. In steel milling applications, coating alterations like wide peening cleaning (WPC) also improved fatigue resistance and prolonged tool life[37]. Additionally, comparative analyses demonstrated that TiAlSiN nanocomposites perform better than AlTiN when titanium alloys are dry milled because they minimize oxidation damage and cracks[2]. Research on cavitation erosion and sliding wear confirms that AlTiN and TiAlN coatings are more durable than bare surfaces[38]. The present study's emphasis on AlCrN and AlTiN systems for high-load, high-temperature wear applications is supported by these findings, which, taken together, highlight the significance of coating composition and processing in tribological performance.

Tool life, surface finish, and wear resistance in harsh machining environments have been greatly improved by developments in hard coatings such as AlTiN, AlCrN, and

Cite: A. Kaur, J. Dureja, J. Grewal, "Enhancing Wear Resistance of EN-19 Steel with Physical Vapor Deposition (PVD) Coatings: Experimental and Statistical Analysis". Evergreen, 13 (02) 517-536 (2026). https://doi.org/10.5109/7420066.

related nanocomposites. Early research highlighted the importance of nanostructured and multilayer coatings; during Ti6Al4V machining, AlTiN/TiN nanolayers and nanocomposites showed enhanced wear resistance and up to four times longer tool life than uncoated tools[5]. Similarly, the addition of Si and multilayer designs enhanced oxidation resistance, adhesion, and hardness; in terms of cutting capability, AlCrSiN coatings exceeded AlTiSiN[4].

It has been demonstrated that surface pre-treatment methods such as Ar ion cleaning in conjunction with adjusted substrate bias greatly improve adhesion and lower wear rates of AlTiSiN coatings[39]. AlTiN/a-Si3N4 nanocomposite coatings also enhanced drilling performance by lowering surface roughness and flank wear[40]. When AlTiN, AlCrN, and DLC coatings were compared, it was found that multilayer AlCrN gave boiler steels the best erosion resistance under hot conditions[41]. Additionally, during Inconel 718 machining, the addition of Ni to AlTiN coatings improved toughness and decreased adhesion wear[35]. Additionally, compared to traditional oxide-based coatings, industrial investigations demonstrated that nano-multilayer AlTiN/TiN coatings prevented fracture widening and more than doubled tool life[33]. These investigations demonstrate the direct effects of alloying, pre-treatment, and coating architecture on wear mechanisms, which is consistent with the current study's emphasis on AlCrN and AlTiN systems for enhanced tribological applications.

One of the most critical areas of research in machining applications has been the effectiveness of improved coatings in improving tool life and wear resistance[42]. showed that in micro-milling Ti6Al4V, where abrasion predominated as the primary wear mechanism, nano-crystalline diamond (NCD) coatings offered better burr control but showed higher wear in comparison to AlCrN and TiN coatings. Similarly[43], showed that TiN/AlTiN and AlTiN/TiN nanomultilayer coatings exhibited strong tribological properties, with coating architecture influencing hardness and wear performance.

Impact testing and structural alterations have also been used to optimize coatings[1]. These methods demonstrated the load sensitivity of TiN and AlTiN coatings, demonstrating that non-columnar microstructures enhanced impact resistance at lower loads but restricted ductility at higher stresses. The hardness and wear resistance of AlCrSiN-based nanocomposite coatings alloyed with Mo and Nb were found to be superior to those of standard AlCrN during Inconel 718 machining[6].

Furthermore, high-temperature wear behavior on Ti-6Al-4V alloys was significantly improved by hybrid coatings that combined AlCrN and DLC, with DLC showing better hardness and less delamination[44]. The current research into AlCrN and AlTiN coatings for tribological applications is directly supported by these works, which collectively demonstrate the importance of coating architecture, alloying, and testing conditions in determining wear performance.

Recent studies have highlighted the significance of surface engineering and hybrid manufacturing approaches in enhancing the mechanical and tribological properties of advanced materials[45]. Similarly, hardfacing processes employing TIG welding with Stellite-6 as a thermal spraying substrate have been shown to significantly improve surface hardness and the wear resistance of alloy steels under extreme service conditions[45]. Furthermore, FDM-assisted investment casting was applied to fabricate Al–Al_2O_3 composites with simultaneous improvements in hardness, surface finish, and wear resistance[45].

Machine learning (ML) techniques have emerged as highly effective tools for process optimization and predictive modelling[46]. Studies on TiB_2-reinforced Al6061 composites have established that increasing reinforcement content enhances tensile strength and hardness, with significant implications for tribological applications[47]. The flexural strength and fracture behavior of ABS–Al composites have also been improved[48].

Nano-sized ceramic particle reinforcement and cooling agents have shown promise in enhancing fracture toughness and wear resistance in Al7075-based hybrid composites, aligning with ongoing efforts to minimize material loss under dry sliding conditions[49]. ML-driven strength modeling of ABS/glass fiber sandwich composites has revealed infill density and nozzle temperature as the most critical parameters influencing mechanical properties[50]. Beyond coatings, non-conventional machining techniques have been proposed as viable options for processing Monel-400 with reduced tool wear and energy costs, for difficult-to-machine alloys[51]. The research on slurry erosion in WC-Co and Cr_3C_2-NiCr coatings for hydro turbine steels emphasizes the importance of appropriate process parameter selection to achieve superior erosion performance, offering significant implications for the long-term durability of components in hydropower applications[52].

2. Materials and Methodology

EN-19 alloy steel was selected as the substrate due to its widespread use in Rzeppa-type automotive CV joints. The chemical composition conforms to the EN-19 standard: C, 0.410%; Cr, 0.920%; Mo, 0.170%; Mn, 0.83%; P, 0.017%; S, 0.011%; balance Fe. Spherical EN-31 steel counter-bodies were used during wear tests due to their high carbon content, excellent hardness, and commercial relevance in CV joint ball-track interactions. This coupling replicates actual drivetrain sliding-pair material combinations and maintains consistent abrasion and contact-stress conditions. The schematic of the ball-on-disc wear test is shown in Figure 1.

Cite: A. Kaur, J. Dureja, J. Grewal, "Enhancing Wear Resistance of EN-19 Steel with Physical Vapor Deposition (PVD) Coatings: Experimental and Statistical Analysis". Evergreen, 13 (02) 517-536 (2026). https://doi.org/10.5109/7420066.

Table 1: Deposition parameters of AlCrN and AlTiN

Parameters	AlTiN	AlCrN
Layer Type	Mono	Mono
Machine Used	Standard Balzers Rapid Coating System (RCS) Machine	Standard Balzers Rapid Coating System (RCS) Machine
Make	Oerlikon Balzers, Swiss	Oerlikon Balzers, Swiss
Deposition Pressure	3.5 Pa	3.5 Pa
Number of targets	Ti (02), $Ti_{50}Al_{50}$(04)	$Al_{70}Cr_{30}$ (06)
Reactive Gas	Nitrogen	Nitrogen
Coating Thickness	4 µm ± 1 µm	4 µm ± 1 µm
No. of Target	8	8
Targets Composition	Ti, $Ti_{50}Al_{50}$	$Al_{70}Cr_{30}$
Max Service Temperature (ºC)	1000	1100
Coating Hardness H_{IT}(GPa)	35 ± 3	36 ± 3
Substrate bias voltage	-40 V to -170 V	-40 V to -170 V

The high hardness, thermal stability, and shown wear resistance under extreme tribological circumstances led to the selection of two PVD coatings: aluminum titanium nitride (AlTiN) and aluminum chromium nitride (AlCrN). To ensure consistent, thick coatings, DC magnetron sputtering was used to deposit both, with careful control over vacuum, plasma, and substrate biasing as shown in Table 1.

To simulate extreme CV joint conditions, wear experiments were conducted at ambient temperature. At 200°C, an enclosed chamber with thermal shielding prevented accelerated oxidation and maintained stable heat transfer conditions. Steel balls with a diameter of 14 mm were used as counter bodies against rotating discs in a ball-on-disc tribometer with a 60 mm track radius. Test durations were 5, 5, 10, 10,15, 15, and 30 minutes; normal loads were 30, 40, and 50 N; and sliding velocities were 0.5, 1.0, and 2.0 m/s, along with sliding speeds of 96 rpm, 191 rpm, and 382 rpm. Each experimental condition was repeated three times to ensure repeatability. Wear of the coated and uncoated EN-19 discs was quantified by mass loss. Before and after each test, the discs were stabilized to control moisture, then weighed using an analytical electronic balance with a resolution of 0.1 mg. The mass loss for each interval was obtained from the difference between the initial mass and the mass after sliding. For each test condition, three replicate experiments were performed, and the reported values are the mean mass loss, with standard deviations used to indicate scatter in the plots and in Table 2. The cumulative mass loss Δm was converted to volume loss Δv, assuming a constant material density. A density of 7.85 g/cm³ was used, corresponding to EN-19 bearing steels, since the coating thickness is minimal compared to the bulk material, and its contribution to the overall volume is negligible. The volume loss in mm³ was calculated as per equation 1.

$$\Delta v = \Delta m/\rho \qquad (1)$$

Where Δm is the mass loss in grams, and ρ is the density expressed in g/mm³. The values in Table 2 correspond to the average volume loss per condition obtained from the three repeats. For tests conducted at 200 °C, the specimens were allowed to cool to room temperature inside the enclosed chamber before cleaning and weighing, to avoid additional oxidation during handling. No explicit correction for debris oxidation was applied. The good repeatability of the mass-loss data and the relatively short exposure time at 200 °C indicate that any mass change due to oxide formation is small compared with the measured wear loss and does not affect the subsequent statistical modelling.

To evaluate wear performance, volume loss (mm^3) was first measured, and cumulative weight loss (g) was periodically recorded as a secondary indicator of material deterioration. To assess coating efficacy, comparative tests were performed on untreated, AlTiN-coated, and AlCrN-coated steel specimens. To determine the predominant wear mechanisms and evaluate microstructural alterations, a few samples were analyzed using SEM and EDS in addition to quantitative wear data.

A full-factorial matrix was used in the experiment, with coating type serving as the categorical factor and applied

Fig. 1: Schematic of ball-on-disc wear test

Cite: A. Kaur, J. Dureja, J. Grewal, "Enhancing Wear Resistance of EN-19 Steel with Physical Vapor Deposition (PVD) Coatings: Experimental and Statistical Analysis". Evergreen, 13 (02) 517-536 (2026). https://doi.org/10.5109/7420066.

load, sliding velocity, and test time as input variables. This results in unique test conditions. For each condition, three independent repetitions were performed, giving individual ball-on-disc tests. For each combination, the three wear-volume values were averaged, and the resulting value was used in the subsequent statistical analysis.

To minimize potential systematic errors arising from instrument drift and environmental changes, the tests were carried out in a randomized order within coating blocks. For each coating type, the combinations of time, load, and velocity were randomized using the built-in randomization option of the statistical software, and the resulting sequence was followed during testing. In the regression modelling, time, load, and velocity were treated as continuous variables, whereas the coatings were introduced through dummy variables. The complete factorial dataset is shown in the supplementary materials (Table SM1). The full set of test conditions used in this study is summarized in Table 2.

This method enabled analysis of the impact of both individual and combined parameters on wear. To manage non-linearity and stabilize variance, regression analysis using the Box-Cox transformation was employed. The evaluation of six models (λ = 0, 0.5, 0.6, 0.7, 1, 1.2) was conducted using 10-fold cross-validation, R2, adjusted R^2, and anticipated R^2. The best dependable balance between statistical validity and prediction accuracy was offered by the λ = 0.7 model (R^2 = 88.13%, cross-validation R^2 = 87.04%).

The combined effects of time, velocity, and load on wear loss were demonstrated through contour, surface, main effects, and interaction graphs. According to statistical analysis, load and velocity had a secondary impact, while coating type and test length were the main determinants. In addition to confirming AlCrN coatings excellent effectiveness in minimizing wear loss, combining sophisticated statistical modeling with laboratory wear tests provided a predictive framework for optimizing tribological conditions for actual automotive applications.

3. Result and Discussion

3.1. Wear Test Analysis

Wear loss of EN-19 steel under various coating types, sliding velocities, loads, and time durations is shown in Table 2. Uncoated specimens showed the greatest wear at 30, 40, and 50 N with velocities of 0.5–2 m/s and times of 5–30 min, whereas AlCrN and AlTiN coatings significantly reduced material loss. In contrast to 0.033 and 0.032 mm³ for AlTiN and AlCrN, wear in uncoated samples increased from 0.003 mm³ (5 min) to 0.044 mm³ (90 min) at 0.5 m/s and 30 N. Results were also affected by speed; during 90 minutes, coated samples stayed much lower (0.022 for AlCrN, 0.019 for AlTiN) while uncoated samples reached 0.041 mm³ at 2 m/s. Overall, coatings showed better stability under dynamic sliding conditions and better resistance to abrasive and adhesive wear, especially AlCrN.

Table. 2: Experimental matrix: Test time, sliding velocity, load, and coating type used in the wear analysis of EN-19 steel

Time (min)	Sliding Velocity (m/s)	Load (N)	Coating Type
5, 5, 10, 10, 15, 30	0.5, 1, 2	30, 40, 50	Uncoated, AlTiN, AlCrN

Wear loss increases significantly with load when load variation (30N, 40N, 50N) is added at 1 m/s, particularly in uncoated samples. For example, uncoated samples exhibit 0.024–0.030 mm³ wear at 15 min and 50 N, while AlCrN samples exhibit 0.017–0.022 mm³ wear. This shows that while higher loads increase contact stress and accelerate wear, coatings, particularly AlCrN, can effectively withstand higher loads by strengthening the surface and minimizing material transfer.

- Overall, the same pattern can be observed for all combinations of load, velocity, and time:
- Uncoated specimens: Poor endurance and the highest wear.
- AlTiN-coated specimens: Significantly less wear and intermediate performance when compared to uncoated.
- Specimens coated with AlCrN: Best performance, consistently exhibiting the least amount of wear in all circumstances.

Higher loads, longer test times, and higher sliding velocities all resulted in increased wear loss. Uncoated steel displayed the highest wear, but protective coatings significantly increased resistance. AlCrN and AlTiN performed best. AlCrN is therefore the best coating for increasing the longevity of EN-19 steel in tribological applications, such as CV joints and other automotive parts subjected to high sliding conditions and pressures.

3.2. Wear Performance of Samples

Cumulative weight loss under dry sliding conditions at 30 N, 1 m/s, and 200°C is shown in Figure 2. Over time, wear developed significantly; by 30 minutes, the uncoated sample had lost approximately 0.037 g. With final weights of ~0.023 g (AlTiN) and ~0.022 g (AlCrN), representing a roughly 40% reduction, coated specimens fared much better. AlCrN consistently outperformed AlTiN, especially over more extended periods, demonstrating its stronger protective properties.

Cumulative weight loss under dry sliding conditions at 30 N, 0.5 m/s, and 200 °C is shown in Figure 3. Every sample displayed increasing wear; after 30 minutes, the uncoated steel weighed about 0.044 g. Wear was reduced by 25–30% in coated specimens, with AlTiN weighing approximately 0.033g and AlCrN weighing approximately 0.032 g.

Cite: A. Kaur, J. Dureja, J. Grewal, "Enhancing Wear Resistance of EN-19 Steel with Physical Vapor Deposition (PVD) Coatings: Experimental and Statistical Analysis". Evergreen, 13 (02) 517-536 (2026). https://doi.org/10.5109/7420066.

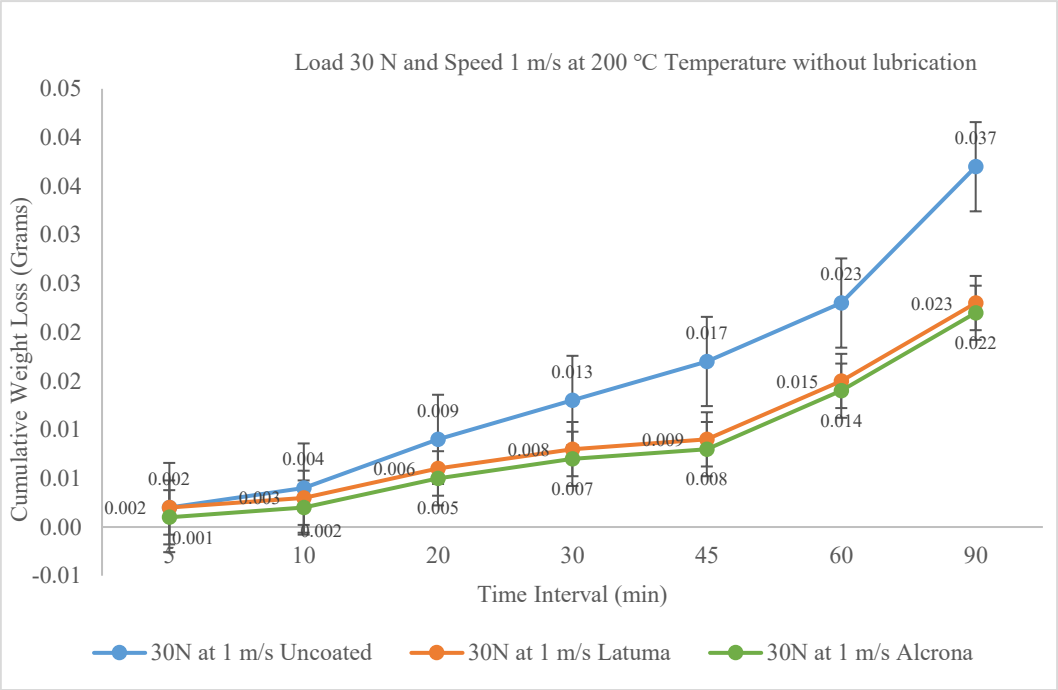

Fig. 2: Cumulative weight loss vs. time at 30 N load and 1 m/s sliding speed under dry conditions at 200 °C

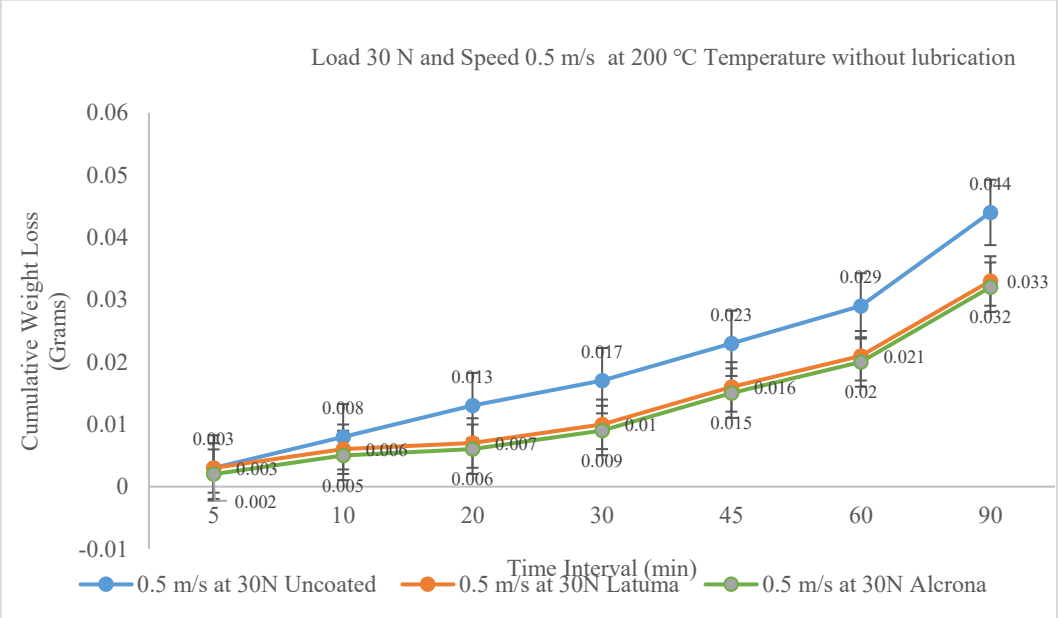

Fig. 3: Cumulative weight loss vs. time at 30 N load and 0.5 m/s sliding speed under dry conditions at 200 °C

Cumulative weight loss under dry sliding conditions at 30 N, 2 m/s, and 200 °C is displayed in Figure 4. Every specimen showed slow wear; after 30 minutes, the uncoated sample weighed about 0.041 g. Wear was significantly reduced by coatings: AlTiN reached about 0.022 g and AlCrN about 0.019 g, indicating improvements of 45–55%. AlCrN consistently outperformed AlTiN, demonstrating superior protection at high temperatures and speeds.

Cumulative weight loss under dry sliding conditions at 40 N, 1 m/s, and 200 °C is shown in Figure 5. Both coatings considerably decreased material loss to ~0.034 g (AlTiN) and ~0.033 g (AlCrN), a 25–30% improvement. In contrast, the uncoated steel displayed the maximum wear, reaching ~0.045 g at 30 minutes. Despite AlCrN's slightly superior performance, the coating differences were negligible. These findings support the usefulness of coatings in prolonging surface life under increased load circumstances.

Cumulative weight loss under dry sliding conditions at 50 N, 1 m/s, and 200 °C is displayed in Figure 6. The coated samples showed decreased wear: ~0.038 g (AlTiN) and ~0.035 g (AlCrN), a 20–25% reduction, but the uncoated

Cite: A. Kaur, J. Dureja, J. Grewal, "Enhancing Wear Resistance of EN-19 Steel with Physical Vapor Deposition (PVD) Coatings: Experimental and Statistical Analysis". Evergreen, 13 (02) 517-536 (2026). https://doi.org/10.5109/7420066.

specimen reached ~0.047 g at 30 minutes, suggesting severe damage. AlCrN showed reduced wear at all intervals, consistently outperforming AlTiN. Although wear still increases with load, these data demonstrate that protective coatings, particularly AlCrN, improve durability under high-load, dry, and high-temperature environments.

3.3. Regression Analysis

A quantitative relationship between process variables (load, sliding velocity, and time) and the wear loss of EN-19 steel samples, both coated and uncoated, was established using regression analysis. The model improved prediction reliability by stabilizing variance and accounting for nonlinearities in the data through multiple linear regression and a Box–Cox transformation. Statistical metrics such as R^2, adjusted R^2, and predicted R^2 confirmed the adequacy of the model, while residual and normal probability plots confirm error distribution. This enabled the regression equation to forecast performance in untested situations and highlighted the key elements influencing wear. Thus, the regression analysis's results provided a strong predictive framework for comparing the protective effectiveness of AlTiN and AlCrN coatings on EN-19 steel and for selecting the optimal tribological conditions.

The experimental design matrix describing the combination of test parameters considered in the investigation is shown in Table 2. In addition to the coating type (uncoated, AlTiN, or AlCrN), the table contains three important input variables: time (minutes), sliding velocity (m/s), and applied load (N). The ball-on-disc tribometer

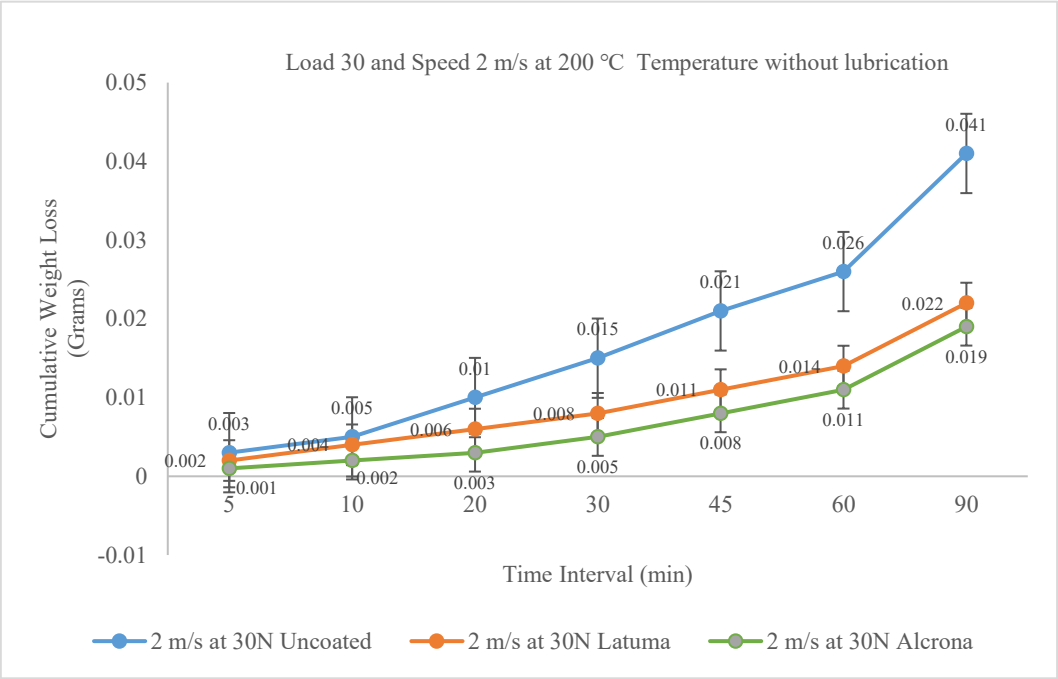

Fig. 4: Cumulative weight loss vs. time at 30 N load and 2 m/s sliding speed under dry conditions at 200 °C

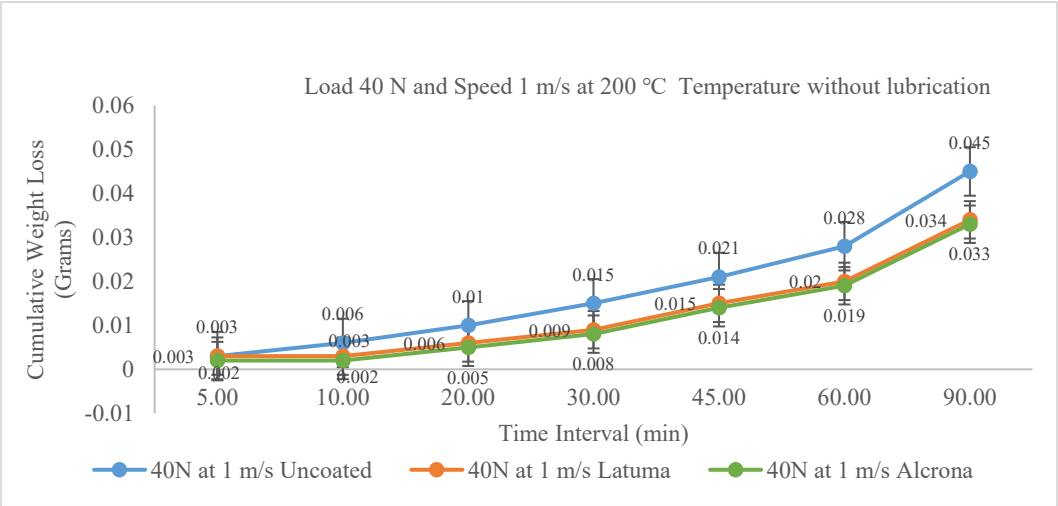

Fig. 5: Cumulative weight loss vs. time at 40 N load and 1 m/s sliding speed under dry conditions at 200 °C

Cite: A. Kaur, J. Dureja, J. Grewal, "Enhancing Wear Resistance of EN-19 Steel with Physical Vapor Deposition (PVD) Coatings: Experimental and Statistical Analysis". Evergreen, 13 (02) 517-536 (2026). https://doi.org/10.5109/7420066.

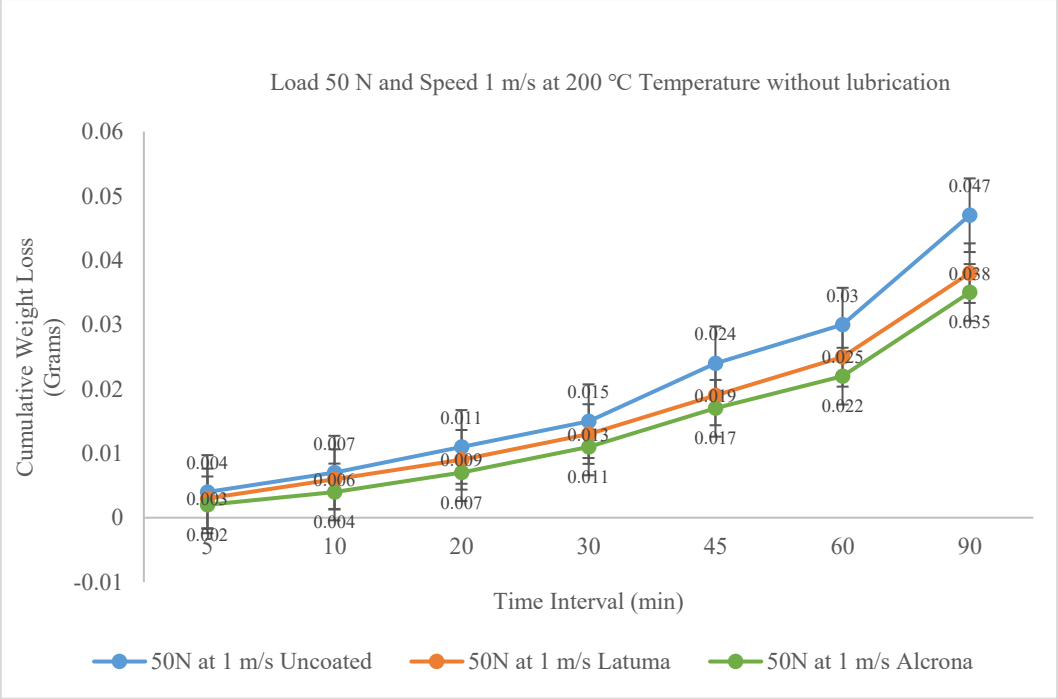

Fig. 6: Cumulative weight loss vs. time at 50 N load and 1 m/s sliding speed under dry conditions at 200 °C

Table. 3: Model comparison using Box–Cox transformations with statistical measures and cross-validation results

Sr. No	Model	Model Summary for Transformed Response					
		S	R-sq	R-sq(adj) %	R-sq(pred) %	10-fold S	10-fold R-sq%
Model-1	Method Box-Cox transformation Rounded λ 0.5 Estimated λ 0.588995 95% CI for λ (0.442495, 0.731495) Cross-validation 10-fold	0.017	86.59	86.05	85.14	0.017	85.45
Model-2	Method Box-Cox transformation λ = 0.6 Cross-validation 10-fold	0.013	87.52	87.02	86.15	0.013	86.43
Model-3	Method Box-Cox transformation λ = 0.7 Cross-validation 10-fold	0.009	88.13	87.66	86.79	0.009	87.04
Model-4	Method Box-Cox transformation λ = 1.2 Cross-validation 10-fold	0.002	87.26	86.75	85.54	0.002	85.67
Model-5	Method Box-Cox transformation λ = 0 Cross-validation 10-fold	0.457	77.00	76.09	74.55	0.466	74.90
Model-6	Method Box-Cox transformation λ = 1 Cross-validation 10-fold	0.003	88.29	87.83	86.82	0.004	86.99

was used to measure wear loss (mm^3) under each test condition, which is represented by a different row. Regression modeling is based on tabular data because it consistently captures changes in wear in relation to changing factors. Higher loads and velocities, for instance, capture more severe wear scenarios, whereas tests conducted at low loads and velocities offer a baseline of moderate wear. The experimental plan ensures coverage of the entire parameter space, enabling the regression model to detect the primary effects of wear loss (the independent influences of time, load, and velocity) and interaction effects (such as the load–velocity interaction). Therefore, Table 3 provides a crucial connection between the predictive regression model developed in this work and the raw experimental observations.

Comparing all regression models created with Box-Cox

transformations reveals variations in their statistical validity, predictive accuracy, and compliance with regression standards. With R^2 values of 86.59% and 87.52%, respectively, Model-1 ($\lambda = 0.5$) and Model-2 ($\lambda = 0.6$) demonstrated respectable fits; nevertheless, their prediction abilities were marginally less than those of the later models. With an R^2 of 88.13%, a predicted R^2 of 86.79%, and a cross-validation R^2 of 87.04%, Model-3 ($\lambda = 0.7$) fared better than these while keeping the residual standard error (S = 0.00965) extremely low. This showed that Model-3 produced extremely accurate and consistent forecasts, explaining over 88% of the variation in wear loss. Crucially, the Box–Cox confidence interval (0.44–0.73) contains the λ value of 0.7, indicating that the regression conditions of homogeneity of variance and normality of residuals were satisfied. However, Model-6 ($\lambda = 1$) provided the greatest R^2 (88.29%), but it was also beyond the legitimate Box–Cox range, making it statistically weaker because of possible heteroscedasticity or non-normality in residuals. Model-4 ($\lambda = 1.2$) also fell outside the confidence interval. The worst model, Model-5 ($\lambda = 0$, log transformation), has poor predictive performance and only 77% explanatory power. The best balance between accuracy, predictive power, and statistical justification was thus found in Model-3, which was determined to be the most appropriate regression model. This finding was reinforced by the residual analysis, which confirmed the model's reliability by showing tightly clustered residuals around the fitted values. In conclusion, Model-3 with $\lambda = 0.7$ is the best option for interpretation and future use in coating performance optimization, as it offers the most reliable, theoretically supported framework for forecasting wear loss in EN-19 steel under both coated and uncoated conditions.

3.3.1. Regression Equation

The transformed wear is expressed as a function of coating, load, velocity, and time in regression equation 2.

$$Wear\ Loss^{0.7} = 0.011571 + 0.003036\,Time - 0.00577\,Velocity + 0.000436\,Load - 0.00889\,Coating \quad (2)$$

Wear increases with longer test durations and greater applied loads, as indicated by the positive coefficients for time (0.003036) and load (0.000436). On the other hand, velocity exhibits a negative coefficient (-0.00577), indicating that wear is reduced at higher sliding speeds, perhaps due to the formation of a protective tribo-layer. The efficiency of AlTiN and AlCrN in reducing wear compared to uncoated specimens is confirmed by the negative coating coefficient (−0.00889), with Alcrona providing the best protection.

3.3.2. Coefficients for Transformed Response

Table 4 shows that time has the largest t-value (25.64, p = 0.000), indicating it is the most significant characteristic. Wear increases significantly over more extended periods. Higher loads accelerate wear, as seen by the significant positive effect of load (t = 3.66, p = 0.000). The adverse impact of velocity (t = −2.97, p = 0.004) indicates that wear decreases with increasing speed. Coating has a significant detrimental effect (t = -7.71, p = 0.000), demonstrating its effectiveness in reducing wear. There is no multicollinearity when the VIF value is close to 1.

3.3.3. Model Summary for Transformed Response

The statistical results demonstrate the regression model's high degree of reliability. With a very low standard error of regression (S = 0.00965), the predictions are accurate. The model explains more than 88% of the variation in wear loss, as indicated by the coefficient of determination (R^2 = 88.13%), and its robustness is confirmed by the adjusted R^2 (87.66%), which accounts for predictor effects. Strong generalizability and little overfitting are demonstrated by the tight alignment of the 10-fold cross-validation R^2 (87.04%) and the anticipated R^2 (86.79%). Overall, the model offers outstanding prediction capability and precision for analyzing wear behavior.

3.3.4. Analysis of Variance for Transformed Response

The regression model is statistically significant (F = 185.69, p = 0.000), according to the ANOVA results (Table 5), which also show a good overall fit. Time is the primary variable affecting wear loss, contributing the most among the components (F = 657.24, p = 0.000). Additionally, coating has a significant impact (F = 59.37, p = 0.000), confirming its protective function. While still substantial, load (F = 13.39, p = 0.000) and velocity (F = 8.81, p = 0.004) have less of an impact. The model still successfully captures the main trends, but the significant lack of fit (p = 0.003) indicates some unexplained variation. The lack-of-fit analysis (Table 5) indicates a statistically significant lack of fit (p = 0.003), demonstrating that a purely linear model in time, load, velocity, and coating does not fully capture the curvature of the wear–response surface. To address this, additional models incorporating selected interaction terms (time × load, time × velocity) and a quadratic term in time were evaluated. These extended models showed marginal increases in R^2 (< 2%) but substantially increased model complexity without altering the direction, significance, or physical interpretation of the main effects. Given the goal of maintaining a parsimonious and interpretable predictive framework for coating selection, the linear model with a Box–Cox transformation ($\lambda = 0.7$) was retained, acknowledging its limitations. The residual structure indicates minor curvature at longer sliding durations, suggesting that unmodeled nonlinearities, such as running-

Table. 4: Regression Coefficients for Transformed Wear Loss Response

Term	Coef	SE Coef	T-Value	P-Value	VIF
Constant	0.0157	0.0058	2.68	0.009	
Time (min)	0.003	0.0001	25.64	0	1
Velocity (m/s)	-0.006	0.0019	-2.97	0.004	1
Load (N)	0.0004	0.0001	3.66	0	1
Coating	-0.009	0.0011	-7.71	0	1

Table. 5: ANOVA for Transformed Wear Loss Response

Source	DF	Adj SS	Adj MS	F-Value	P-Value
Regression	4	0.069189	0.017297	185.69	0.000
Time (min)	1	0.061223	0.061223	657.24	0.000
Velocity (m/s)	1	0.000820	0.000820	8.81	0.004
Load (N)	1	0.001248	0.001248	13.39	0.000
Coating	1	0.005531	0.005531	59.37	0.000
Error	100	0.009315	0.000093		
Lack-of-Fit	55	0.006837	0.000124	2.26	0.003
Pure Error	45	0.002478	0.000055		
Total	104	0.078504			

in effects or tribo-layer evolution, may contribute to the observed deviations.

The negative coefficient associated with sliding velocity must be interpreted cautiously. Although higher speeds can, in some systems, promote the formation of a protective tribo-layer due to thermal and chemical stabilization, the present study lacks SEM/EDS evidence collected explicitly at different velocities. Therefore, this observation is treated as a hypothesis consistent with the literature rather than a definitive mechanism.

Model validation was performed using a 10-fold cross-validation procedure, in which the dataset was randomly partitioned into 10 equal subsets; each subset was used once as the test fold, while the remaining 9 formed the training set. The averaged cross-validation R^2 (87.04%) closely matched the predicted R^2 (86.79%), confirming excellent generalizability with minimal overfitting. For completeness, a parity plot (predicted vs. measured wear) with a 45° reference line is recommended to demonstrate model performance, highlighting strong agreement between experimental observations and model predictions.

3.3.5. Fits and Diagnostics for Unusual Observations

The comparison of observed and fitted values demonstrates how accurately the regression model predicts wear loss. The fitted values (0.01907, 0.01183, 0.01541 mm^3) for most observations (such as Obs 46, 48, and 52) are reasonably accurate, with a slight underestimation, and are close to the experimental data (0.029, 0.020, and 0.026 mm^3). In contrast to observed values, the model slightly overpredicts wear in a few cases (Obs 59, 62, 63). Although there may be local variations due to experimental factors not included in the model, overall, the deviations are small, indicating that the regression model accurately reflects the wear behavior patterns.

3.3.6. Residual Plots for Wear Loss (mm^3)

Figure 7 shows residual plots validating the regression model for predicting wear loss. The Normal Probability Plot usually confirms distributed errors, supported by the bell-shaped histogram. Residuals versus Fits indicate homoscedasticity with random scatter around zero, while Residuals versus Order show independence across observations. Together, these diagnostics confirm the model meets statistical assumptions and is reliable for wear-loss prediction.

3.4. Contour and Surface Plots

Figure 8 presents contour and surface plots showing the combined effects of load, velocity, and time on wear loss. Contours illustrate stability, with closely packed bands marking high-wear regions. Load and time dominate, shifting responses toward higher wear at larger values, while velocity plays a secondary role, with slightly lower wear at higher speeds. Surface plots provide 3D visualization: time and load interactions show steep nonlinear rises, whereas velocity interactions appear less significant. Coatings such as AlCrN and AlTiN flatten surfaces and shift responses to low-wear zones, confirming their protective role. Overall, these plots highlight load and time as the critical factors, with coatings effectively enhancing wear resistance, but even under extreme

Cite: A. Kaur, J. Dureja, J. Grewal, "Enhancing Wear Resistance of EN-19 Steel with Physical Vapor Deposition (PVD) Coatings: Experimental and Statistical Analysis". Evergreen, 13 (02) 517-536 (2026). https://doi.org/10.5109/7420066.

operating conditions, degradation still accelerates.

3.5. Mean Effects Plot for Wear Loss

The primary effects of time, velocity, load, and coating on wear loss (mm3) are shown in Figure 9. Time is the primary factor, as wear increases significantly with test duration. A modest downward trend in velocity suggests that higher speeds might encourage protective tribolayers. As contact pressures increase from 30 to 50 N, the load causes a slight increase in wear. The type of coating is also important; untreated samples perform the worst, while AlCrN and AlTiN provide the highest protection. In general, coating and time have the most impact, while load and velocity have less significant effects.

3.6. SEM/EDAX of Worn-Out Samples

Results of SEM-EDAX elemental analysis of coated EN-19 steel surfaces is shown in Figure 10 and Figure 11. A steel-rich surface with protective elements is indicated by the dominant presence of Fe (52.39%), Cr (11.86%), and Ni (5.70%) in Figure (a), together with moderate quantities of Al and O. Figure (b) shows lower Al, indicating poorer coating adhesion, but higher Fe (55.83%) and Cr (12.64%). The well-formed AlTiN layer in Figure (c) is significantly different, with Ti (31.86%) and Al (17.00%) predominating and Fe (21.74%) being reduced. Lastly, a uniform AlTiN/AlCrN mixed coating is confirmed in Figure (d), which shows a balanced distribution of Al (22.77%), Ti (27.32%), and Fe (26.92%). Overall, the data support the successful deposition of protective PVD coatings. The substantial addition of Ti, Al, and Cr improves surface hardness and resistance to wear, and the coated layers lower Fe content shows that the steel substrate is effectively covered

The EDS analysis further supports the tribological mechanisms inferred from SEM observations. The worn surfaces of both AlTiN- and AlCrN-coated specimens exhibit increased oxygen content, confirming tribo-oxidation during sliding. However, significant differences were observed between the coatings.

On AlTiN, the detected O–Al–Ti signals indicate formation of aluminium and titanium oxides (Al_2O_3 / TiO_2). Still, their irregular distribution and the presence of exposed substrate peaks suggest a non-uniform, weakly protective tribofilm. This correlates with evidence of crack-assisted coating removal under high load.

AlCrN-coated surfaces show a consistently higher Cr and O presence, indicating the development of Cr_2O_3-rich tribo-oxide layers. Chromium oxides are well-known for their:

- high thermochemical stability
- strong adhesion to nitride coatings
- excellent hardness and resistance to shear

The compact and adherent nature of these Cr-rich oxides inhibits further material removal, which explains the lower wear volumes and reduced delamination observed for AlCrN under severe loading. Thus, the superior wear resistance of AlCrN can be attributed not only to its higher intrinsic hardness but also to the formation of a stable protective tribo-film during sliding contact.

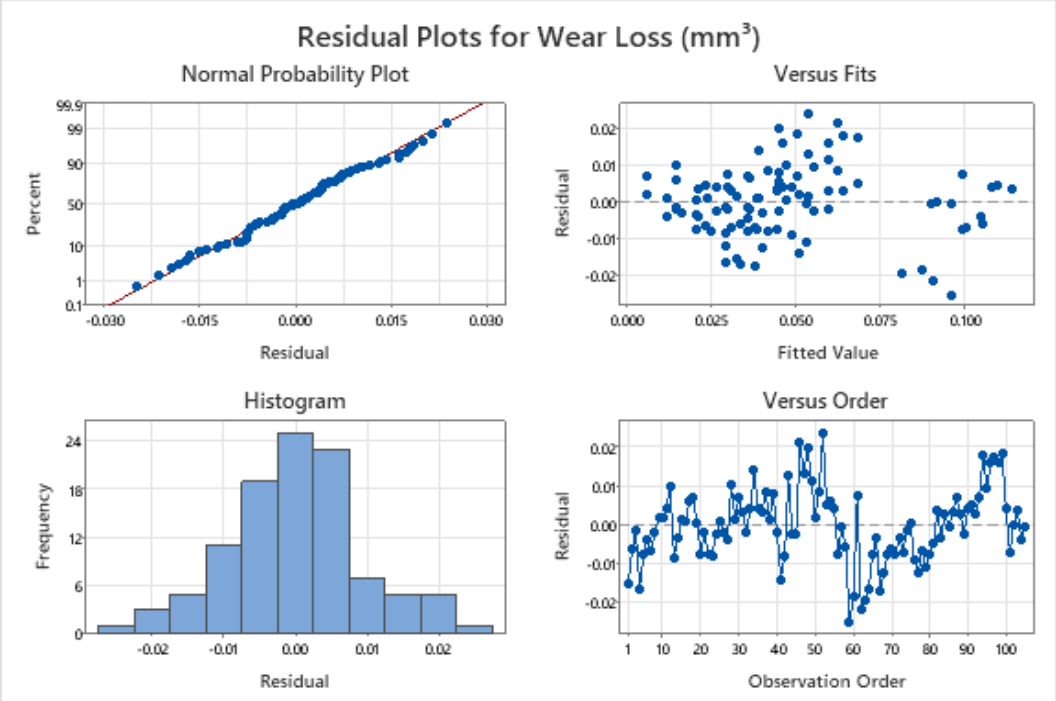

Fig. 7: Residual diagnostic plots for transformed wear loss model

Cite: A. Kaur, J. Dureja, J. Grewal, "Enhancing Wear Resistance of EN-19 Steel with Physical Vapor Deposition (PVD) Coatings: Experimental and Statistical Analysis". Evergreen, 13 (02) 517-536 (2026). https://doi.org/10.5109/7420066.

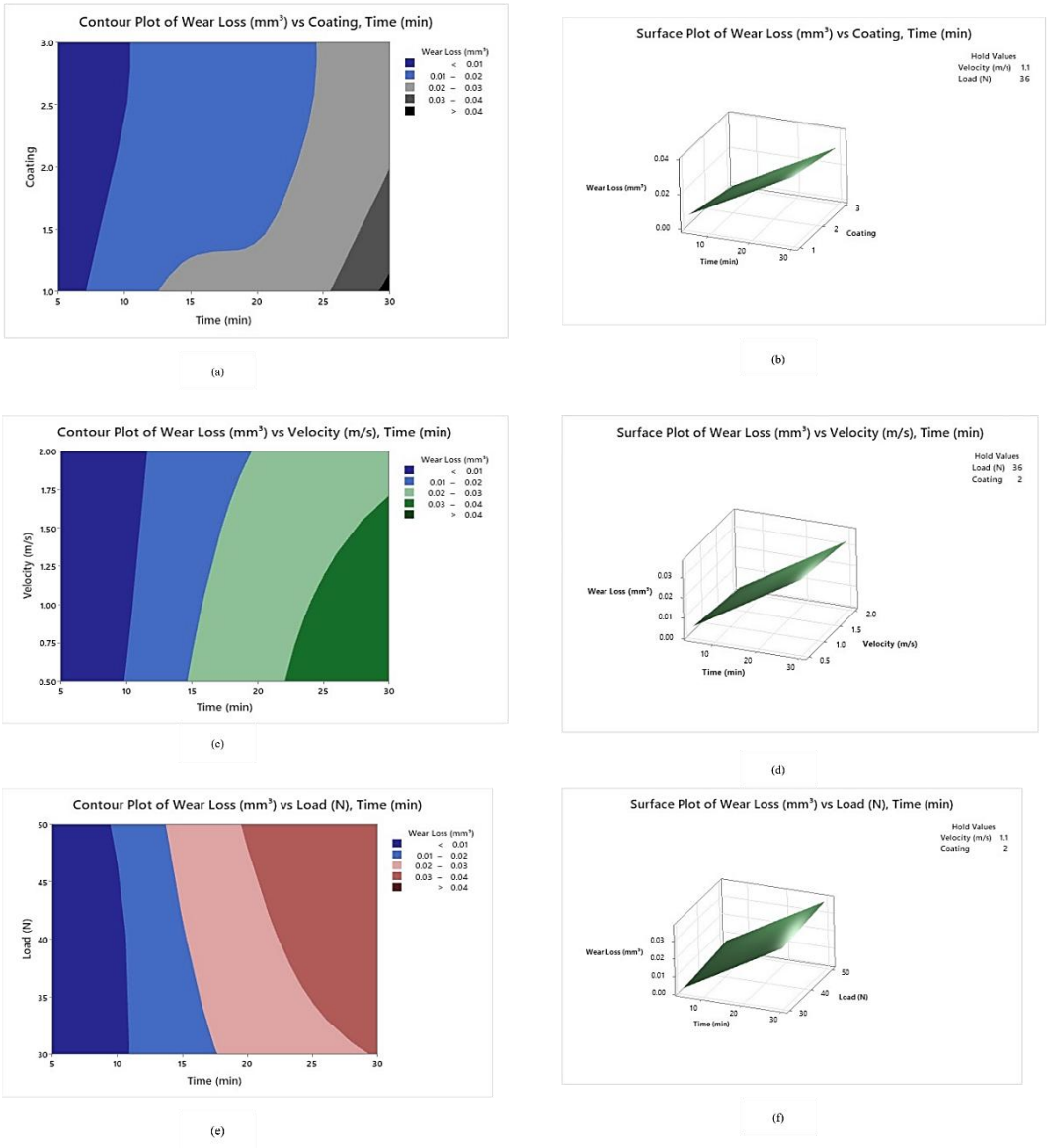

Fig. 8: Wear Loss: (a) Contour Plot of Coating vs. Time, (b) Surface Plot of Coating vs. Time (min), (c) Contour Plot of Velocity (m/s) vs. Time (min), (d) Surface Plot of Velocity (m/s) vs. Time (min), (e) Contour Plot of Load (N) vs. Time (min), (f) Surface Plot of Load (N) vs. Time (min)

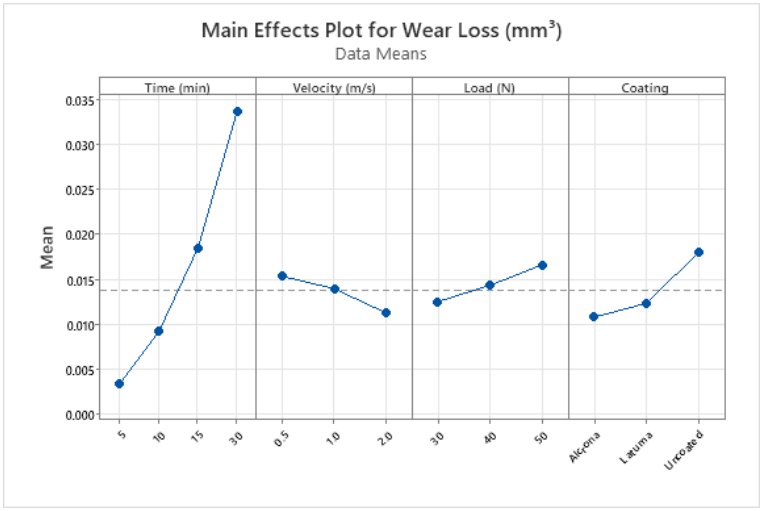

Fig. 9: Main Effects Plot for Wear Loss (mm^3)

Cite: A. Kaur, J. Dureja, J. Grewal, "Enhancing Wear Resistance of EN-19 Steel with Physical Vapor Deposition (PVD) Coatings: Experimental and Statistical Analysis". Evergreen, 13 (02) 517-536 (2026). https://doi.org/10.5109/7420066.

3.7. Interaction Plots for Wear Loss

The effects of time, velocity, load, and coating on wear loss are shown in Figure 12. Time is the most significant factor; regardless of the other factors, wear increases consistently from 5 to 30 minutes. The effect of time, velocity, load, and coating on wear loss is shown in Figure 11. The type of coating is also important. Uncoated specimens perform worst, particularly under higher loads and for more extended periods, while AlCrN and AlTiN consistently exhibit the least wear. Overall, coating and time have the most significant effects, with load and velocity having minor but discernible effects.

3.8. Comparison with Existing Literature

The present study reports a 55% reduction in wear loss for AlCrN-coated EN-19 steel compared with the uncoated substrate. This value is consistent with or superior to improvements reported in recent tribology literature on coated and composite systems. For example Aherwar[53] observed significant wear reduction in TiB_2–CDA/Al6061 hybrid composites by optimizing the reinforcement and sliding conditions. However, their improvements

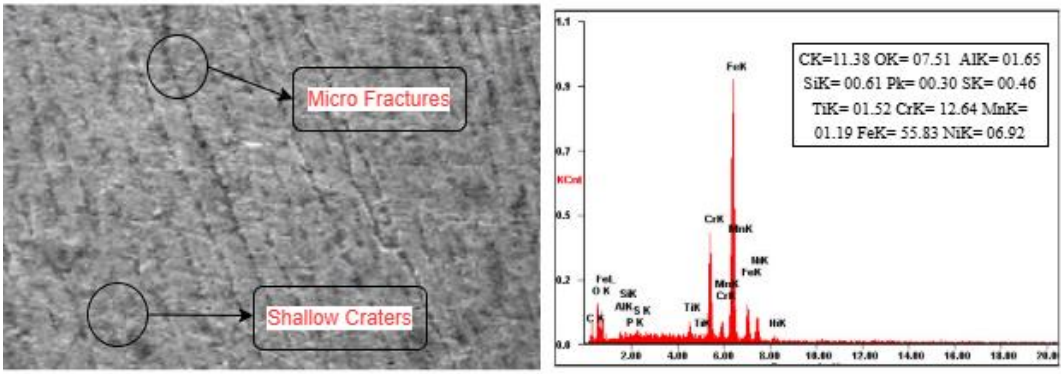

Fig. 10: SEM micrographs with EDS analysis of worn AlCrN-coated EN-19 steel surfaces tested at a constant sliding velocity of 1 m/s: (a) 30 N, (b) 40 N, and (c) 50 N with magnification at x1000 and a 10 µm scale bar

Cite: A. Kaur, J. Dureja, J. Grewal, "Enhancing Wear Resistance of EN-19 Steel with Physical Vapor Deposition (PVD) Coatings: Experimental and Statistical Analysis". Evergreen, 13 (02) 517-536 (2026). https://doi.org/10.5109/7420066.

depended strongly on reinforcement fraction and did not generally exceed the reductions observed with AlCrN in the present work. Similarly, Kumar and Kumar[54] achieved notable decreases in wear rate for hybrid aluminium matrix composites reinforced with ZrB_2 and fly ash; however, their ANN-predicted deviations (0–1.39%) indicated more modest improvements under elevated temperature conditions compared with the strong high-temperature (200 °C) stability exhibited by AlCrN in this study.

For coated steels, Kupczyk[55] demonstrated that TiN$_{0.85}$–Ti coatings effectively mitigated adhesive wear in gear-shaper cutters, thereby improving tool life under high-speed machining. Still, their study did not include elevated-temperature sliding. In contrast, the AlCrN coating examined here maintained significantly lower wear rates even at 200 °C, aligning more closely with the requirements of drivetrain components subjected to thermal and mechanical cycling. Studies on fibre-reinforced composites also report improved tribological performance through NaOH treatment and optimized microstructural design, but the specific wear rate reductions in those systems, while meaningful, generally fall short of the high wear resistance observed for AlCrN. Their polymer-based matrices are not directly comparable to automotive-grade alloy steels under high-load sliding[56,57].

The predictive model developed in this study identifies a practical safe operating window based on time–load–

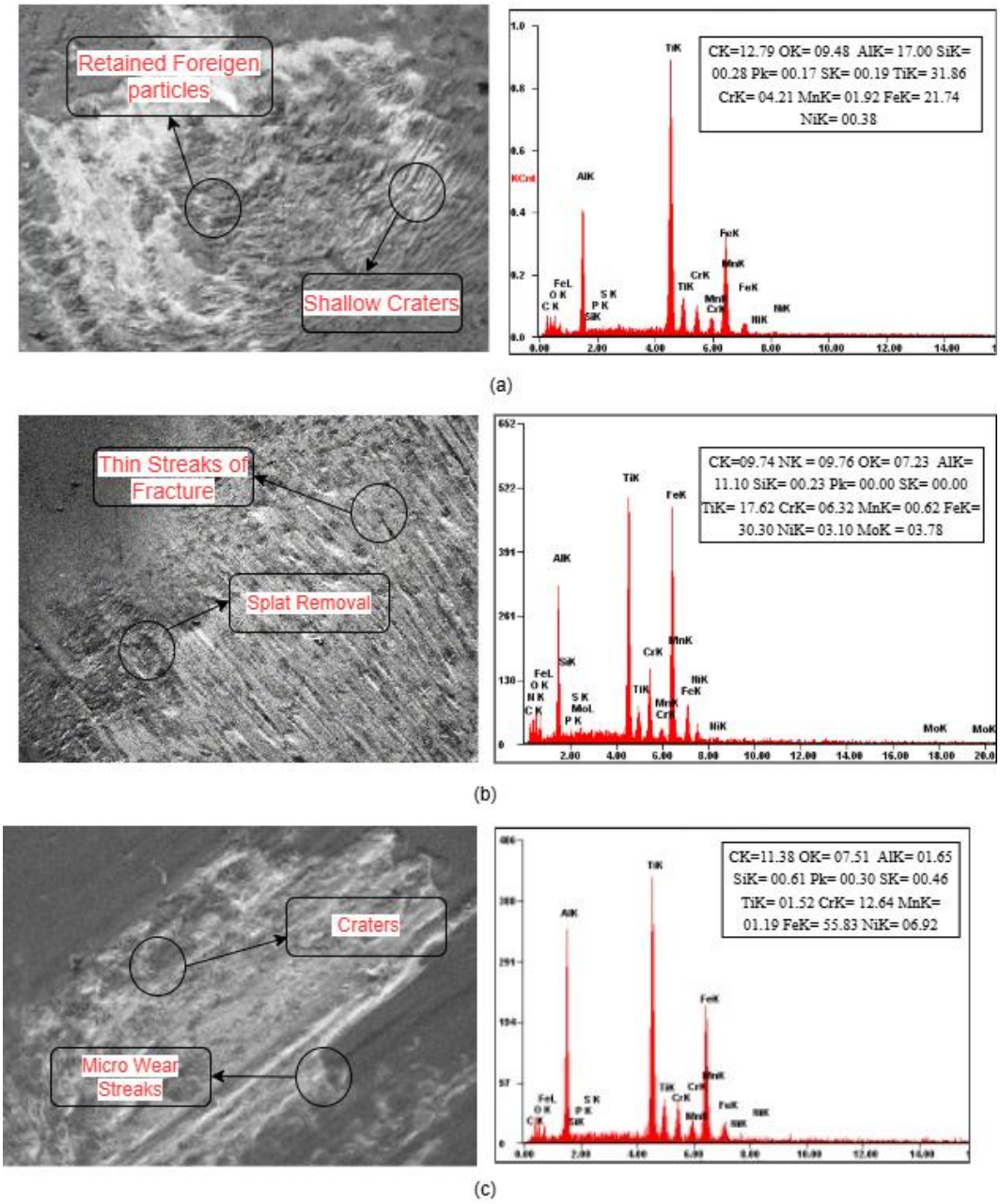

Fig. 11: SEM micrographs with EDS analysis of worn AlTiN -coated EN-19 steel surfaces tested at a constant sliding velocity of 1 m/s: (a) 30 N, (b) 40 N, and (c) 50 N with magnification at x1000 and a 10 µm scale bar

Cite: A. Kaur, J. Dureja, J. Grewal, "Enhancing Wear Resistance of EN-19 Steel with Physical Vapor Deposition (PVD) Coatings: Experimental and Statistical Analysis". Evergreen, 13 (02) 517-536 (2026). https://doi.org/10.5109/7420066.

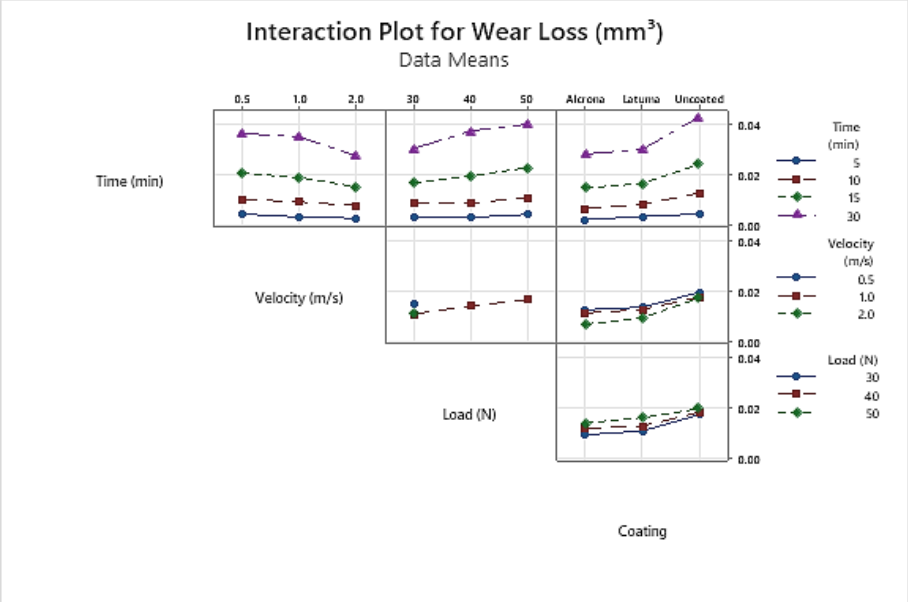

Fig. 12: Interaction Plot for Wear Loss (mm^3)

velocity combinations, showing that wear remains minimal at moderate velocities (1 m/s) and loads up to 40 N for durations of less than 20 minutes. While machine learning–based methods such as Gaussian Process Regression [57] and ANN frameworks have been successfully applied to predict wear in composites, the present Box–Cox–enhanced regression model offers a more straightforward, interpretable, and experimentally validated tool suitable for coated steel systems[54,56]. Thus, the combined experimental and modeling results presented here provide a clearer understanding of wear behaviour under elevated temperature and automotive-relevant sliding conditions, highlighting the strong comparative performance of AlCrN coatings.

3.9. Implications of the Study

The findings of this study have significant scientific, industrial, and sustainability-related implications. The experimental results show that both AlCrN and AlTiN coatings significantly reduce wear on EN-19 steel across a wide range of loads, speeds, and sliding durations. This improvement offers manufacturers a practical way to extend the service life of critical automotive parts, such as CV joints, gears, and shaft components, which often operate under harsh tribological conditions. The observed reduction in wear loss of up to 50–55% for AlCrN-coated specimens indicate an estimated 40–50% longer lifespan for these parts when used in actual CV-joint assemblies.

From an engineering standpoint, integrating experimental tribological data with Box–Cox–optimized regression modeling provides a robust predictive framework for wear-life estimation. This framework enables designers to evaluate coating performance under untested operational scenarios and supports more informed decisions regarding coating selection, maintenance scheduling, and component design. The model's predictive capability, reinforced by strong cross-validation performance, also highlights its potential for application to other coated systems beyond the present study.

The results have broader sustainability implications, in alignment with the Green Asia Strategy. Extending component life directly reduces the frequency of part replacement. Thereby lowering demand for alloy steel extraction, forging, machining energy, and associated transportation. Reduced replacement cycles also translate into lower solid-waste generation from worn-out components. Furthermore, the enhanced wear resistance provided by PVD coatings enables automotive engineers to explore lightweight drivetrain designs. As a result, components can be manufactured with smaller safety margins without compromising durability, and even modest mass reductions in drivetrain assemblies can improve vehicle fuel efficiency and reduce CO_2 emissions over the vehicle's lifetime.

The study demonstrates that advanced PVD coatings such as AlCrN and AlTiN not only improve the tribological performance of EN-19 steel but also support industrial goals of reliability, efficiency, and sustainability. By reducing material loss, energy consumption, and environmental burden, these coatings offer a practical pathway toward greener automotive systems and more resource-efficient manufacturing practices.

4. Conclusions

The wear behavior of EN-19 steel under various tribological conditions, with and without protective coatings of AlTiN and AlCrN, was systematically examined in this study. The findings clearly showed that, across all test settings, uncoated specimens exhibited the highest wear, whereas coated specimens, especially those

Cite: A. Kaur, J. Dureja, J. Grewal, "Enhancing Wear Resistance of EN-19 Steel with Physical Vapor Deposition (PVD) Coatings: Experimental and Statistical Analysis". Evergreen, 13 (02) 517-536 (2026). https://doi.org/10.5109/7420066.

containing AlCrN, consistently showed superior wear resistance. Time, load, and velocity all had an impact; wear loss increased noticeably with higher loads and longer durations, while velocity had a relatively small effect and often contributed to less wear at higher values due to the potential formation of protective tribo-layers.

Model-3 ($\lambda = 0.7$), which offers significant predictive potential with excellent accuracy and adherence to regression assumptions, was shown to be the best model using regression with the Box–Cox transformation. Plots of complementary contours, surfaces, and interactions demonstrated that time and coating type are the primary determinants of wear, with load and velocity having secondary impacts. The substantial wear reduction achieved through AlCrN and AlTiN coatings suggests longer component durability, reduced material consumption, and decreased replacement frequency, aligning the outcomes of this study with global sustainability goals and regional "Green Asia" strategies.

The results show that AlCrN coatings provide the best protection, prolonging component operating life by up to 55% in severe conditions compared to uncoated steel. In applications like CV joints and other automotive parts where endurance under high load and temperature is crucial, these insights offer helpful direction for coating selection and optimization.

5. Limitations and Future Scope

5.1. Limitations

This study has several limitations. The controlled ball-on-disc tests may not accurately replicate the intricate multi-axial loading and lubrication of CV joints. Without taking into consideration cyclic or fluctuating thermal settings, the experiments were restricted to a single temperature (200 °C). Only two PVD coatings, AlTiN and AlCrN, were assessed; multilayer and advanced nanocomposite alternatives were not included. Finally, wear volume was the focus, with little attention paid to variables like coefficient of friction, surface roughness progression, and microstructural changes.

5.2. Future Scope

Future research could use lubricated, cyclic, and impact-loading tests to replicate actual vehicle conditions better. Greater durability may be achievable with more extensive coating options, such as multilayer, plated, or hybrid systems. Thorough microstructural investigations (SEM, TEM, XRD, EDS) provide insight into tribo-film formation and wear mechanisms. While sustainability and life-cycle cost assessments would highlight the broader industrial and environmental benefits of coating EN-19 steel for automotive applications, larger datasets and machine learning could improve predictive models.

Acknowledgement

The facilities and technical assistance provided by Guru Nanak Dev Engineering College in Ludhiana and Punjabi University in Patiala are greatly appreciated by the authors. The Department of Mechanical Engineering deserves special recognition for providing access to the ball-on-disc tribometer and associated facilities. We truly appreciate the help of laboratory personnel with specimen preparation, coating deposition, and wear testing, as well as the advice of mentors and colleagues.

Nomenclature

t	time (min)
v	sliding velocity (m/s^{-1})
F	applied normal load (N)
WL	wear loss (mm^3)
S	standard error of regression (–)
R^2	coefficient of determination (–)
Greek symbols	
λ	Box–Cox transformation parameter (–)
Subscripts	
fit	fitted value
obs	observed value

References

1) J. Chen, H. Li, and B.D. Beake, "Load sensitivity in repetitive nano-impact testing of tin and altin coatings," Surf. Coatings Technol., 308 289–297 (2016). doi:10.1016/j.surfcoat.2016.05.094.
2) J. Liu, S.-S. Zhu, X. Deng, J.-Y. Liu, Z.-P. Wang, and Z. Qu, "Cutting performance and wear behavior of altin- and tialsin-coated carbide tools during dry milling of ti–6al–4v," Acta Metall. Sin. (English Lett., 33 (3) 459–470 (2020). doi:10.1007/s40195-020-01010-6.
3) J.Y. Yi, K.H. Chen, Y.C. Xu, and C.J. Zhu, "Performance of altibn and altitan coatings during milling of titanium," Surf. Eng., 35 (6) 501–506 (2019). doi:10.1080/02670844.2018.1479624.
4) W. Chen, D. Zhang, D. Yao, S. Zhang, and W. Wu, "Investigations on microstructure and mechanical properties of containing-si coatings," Surf. Eng., 33 (7) 536–541 (2017). doi:10.1080/02670844.2017.1287837.
5) H. Çalişkan, E. Altas, and P. Panjan, "Study of nanolayer altin/tin coating deposition on cemented carbide and its performance as a cutting tool," J. Nano Res., 47 1–10 (2017). doi:10.4028/www.scientific.net/JNanoR.47.1.
6) Y. Chen, H. Du, M. Chen, J. Yang, J. Xiong, and H. Zhao, "Structure and wear behavior of alcrsin-based coatings," Appl. Surf. Sci., 370 176–183 (2016). doi:10.1016/j.apsusc.2015.12.027.
7) C. Claudin, J. Rech, W. Grzesik, and S. Zalisz,

"Characterization of the frictional properties of various coatings at the tool/chip/workpiece interfaces in dry machining of aisi 4140 steel," Int. J. Mater. Form., 1 (SUPPL. 1) 511–514 (2008). doi:10.1007/s12289-008-0172-3.

8) J. Rech, C. Claudin, W. Grzesik, and S. Zalisz, "Characterization of the friction properties of various coatings at the tool-chip-workpiece interfaces in dry machining of aisi 4140 steel," Proc. Inst. Mech. Eng. Part J J. Eng. Tribol., 222 (4) 617–627 (2008). doi:10.1243/13506501JET416.
9) B. Podgornik, and J. Vižintin, "Influence of substrate pretreatment on the tribological properties of hard coatings," Stroj. Vestnik/Journal Mech. Eng., 47 (4) 152–162 (2001). https://www.scopus.com/inward/record.uri?eid=2-s2.0-0034790775&partnerID=40&md5=c98f114cc3d9fba598e2f3f36f36e12c.
10) G. Burshukova, A. Kanazhanov, R. Abuova, and A. Joldassov, "Analysis of using damping alloys to improve vibration and strength characteristics in the automotive industry," Evergreen, 10 (2) 742–751 (2023). doi:10.5109/6792824.
11) V. Dubey, K. Pandey, H. Kumar, P.K. Kumar Arora, J.K. Katiyar, and A.K. Sharma, "Tribological behaviour of aisi 304 steel on electrodeposited hard chrome coated steel," Evergreen, 11 (2) 1210–1215 (2024). https://www.scopus.com/inward/record.uri?eid=2-s2.0-85198339375&partnerID=40&md5=c5c8f12e04fa66ab219ff73720f35288.
12) H.S. Grover, S. Deswal, and A. Adhikari, "Analysis and estimation of atmospheric corrosivity of zinc protective coating on steel substrate," Evergreen, 11 (3) 1753–1762 (2024). doi:10.5109/7236827.
13) Y. Mohd-Azmi, F. Ahmad, S. Kabir, N. Nosbi, Y.G. Heng, and A. Zulfiqar, "Analysis of thermal performance of mica-mineral reinforced intumescent coating for structural steel application," Evergreen, 8 (3) 565–573 (2021). doi:10.5109/4491648.
14) P. Guo, R. Chen, H. Li, W. Yang, K. Nishimura, P. Ke, and A. Wang, "Research progress of pvd anti-tribocorrosion coatings under marine environment," Zhongguo Biaomian Gongcheng/China Surf. Eng., 37 (6) 1–20 (2024). doi:10.11933/j.issn.1007-9289.20231228003.
15) S. Kumar, K.C. Anil, and J. Jayappa, "Solid particle erosion performance of multi-layered carbide coatings (wc-sic-cr3c2)," Evergreen, 10 (2) 813–819 (2023). doi:10.5109/6792833.
16) B. Li, Y. Xu, G. Rao, Q. Wang, J. Zheng, R. Zhu, and Y. Chen, "Tribological properties and cutting performance of altin coatings with various geometric structures," Coatings, 13 (2) (2023). doi:10.3390/coatings13020402.
17) R. Pu, Z. Yu, X. Hao, J. Yan, Z. Han, J. Tan, L. Lu, Z. Chen, and H. Yu, "Effect of si content on microstructure, mechanical properties, and cutting performance of tisin/altin dual-layer coating," J. Manuf. Process., 88 134–144 (2023). doi:10.1016/j.jmapro.2023.01.022.
18) D. Özkan, M.A. Alper Yılmaz, D. Karakurt, M. Szala, M. Walczak, S.A. Bakdemir, C. Türküz, and E. Sulukan, "Effect of aisi h13 steel substrate nitriding on alcrn, zrn, tisin, and ticrn multilayer pvd coatings wear and friction behaviors at a different temperature level," Materials (Basel)., 16 (4) (2023). doi:10.3390/ma16041594.
19) C.G. Sriram, N. Ariharan, and N. Radhika, "Comparative study on machining performance of tialsin, altin/tialsin-coated cutting tools," Trans. Inst. Met. Finish., 101 (2) 79–86 (2023). doi:10.1080/00202967.2022.2095113.
20) M. Alfreider, M. Meindlhumer, T. Ziegelwanger, R. Daniel, J. Keckes, and D. Kiener, "Revealing dynamic-mechanical properties of precipitates in a nanostructured thin film using micromechanical spectroscopy," MRS Bull., 49 (1) 49–58 (2024). doi:10.1557/s43577-023-00549-w.
21) P. Czarniak, K. Szymanowski, P. Panjan, and D. Jarosiewicz, "Influence of wc-co knifes pre-treatment with drag finishing method subjected to tool coatings deposition on blunting process," Wood Mater. Sci. Eng., 19 (2) 391–397 (2024). doi:10.1080/17480272.2023.2248471.
22) P. Czarniak, K. Szymanowski, D. Jarosiewicz, P. Panjan, M. Gloeh, and K. Furmańczyk, "The influence of physical vapor deposition (pvd) coating on the microgeometry of high-speed steel (hss) cutting tools during the machining of wood-based composites," Wood Mater. Sci. Eng., (2024). doi:10.1080/17480272.2024.2392034.
23) D. Dinesh Kumar, K. Amirtharaj Mosas, K. Panda, P. Kuppusami, A. Arivarasan, T. Stimpel-Lindner, and G.S. Duesberg, "Low friction characteristics and tribochemistry analysis of novel altin/a-c based nanocomposite coatings," Appl. Surf. Sci., 678 (2024). doi:10.1016/j.apsusc.2024.161137.
24) K. Zheng, Z. Zhang, L. Zhang, Y. Li, D. Jia, J. Ding, and J. Zheng, "Tailoring the structure and properties of bp-hppms deposited altin/tisin bilayer coatings by duty cycle," Ceram. Int., 51 (21) 33564–33574 (2025). doi:10.1016/j.ceramint.2025.05.087.
25) Q. He, J.M. DePaiva, J. Kohlscheen, B.D. Beake, and S.C. Veldhuis, "Study of wear performance and tribological characterization of altin pvd coatings with different al/ti ratios during ultra-high speed turning of stainless steel 304," Int. J. Refract. Met.

Hard Mater., 96 105488 (2021). doi:10.1016/j.ijrmhm.2021.105488.

26) Q. He, J.M. Paiva, J. Kohlscheen, and S.C. Veldhuis, "A study of mechanical and tribological properties as well as wear performance of a multifunctional bilayer altin pvd coating during the ultra-high-speed turning of 304 austenitic stainless steel," Surf. Coatings Technol., 423 (2021). doi:10.1016/j.surfcoat.2021.127577.
27) D. Özkan, M. Alper Yılmaz, M. Szala, C. Türküz, D. Chocyk, C. Tunç, O. Göz, M. Walczak, K. Pasierbiewicz, and M. Yağcı, "Effects of ceramic-based crn, tin, and alcrn interlayers on wear and friction behaviors of altisin+tisin pvd coatings," Ceram. Int., 47 (14) 20077–20089 (2021). doi:10.1016/j.ceramint.2021.04.015.
28) A. Das, M. Kamal, S.R. Das, S.K. Patel, A. Panda, M. Rafighi, and B.B. Biswal, "Comparative assessment between altin and altisin coated carbide tools towards machinability improvement of aisi d6 steel in dry hard turning," Proc. Inst. Mech. Eng. Part C J. Mech. Eng. Sci., 236 (6) 3174–3197 (2022). doi:10.1177/09544062211037373.
29) G. Fox-Rabinovich, G. Dosbaeva, A. Kovalev, I. Gershman, K. Yamamoto, E. Locks, J. Paiva, E. Konovalov, and S. Veldhuis, "Enhancement of multi-scale self-organization processes during inconel da 718 machining through the optimization of tialcrsin/tialcrn bi-nano-multilayer coating characteristics," Materials (Basel)., 15 (4) (2022). doi:10.3390/ma15041329.
30) D. Geng, H. Li, Z. Chen, Y.X. Xu, and Q. Wang, "Microstructure, oxidation behavior and tribological properties of alcrn/cu coatings deposited by a hybrid pvd technique," J. Mater. Sci. Technol., 100 150–160 (2022). doi:10.1016/j.jmst.2021.06.007.
31) B.S. Bektaş, and G. Samtaş, "Optimisation of cutting parameters in face milling of cryogenic treated 6061 aluminium alloy and effects on surface roughness, wear, and cutting temperatures," Surf. Topogr. Metrol. Prop., 10 (2) (2022). doi:10.1088/2051-672X/ac6c40.
32) A. Roushan, U.S. Rao, P. Sahoo, and K. Patra, "Performance study of uncoated and altin-coated tungsten carbide tools in micromilling of ti6al4v using nano-mql," J. Brazilian Soc. Mech. Sci. Eng., 45 (1) (2023). doi:10.1007/s40430-022-03997-8.
33) L. Zhang, Z.-Q. Zhong, L.-C. Qiu, H.-D. Shi, A. Layyous, and S.-P. Liu, "Coated cemented carbide tool life extension accompanied by comb cracks: the milling case of 316l stainless steel," Wear, 418–419 133–139 (2019). doi:10.1016/j.wear.2018.11.019.
34) Z.R. Liu, Y.X. Xu, B. Peng, W. Wei, L. Chen, and Q. Wang, "Structure and property optimization of ni-containing alcrsin coatings by nano-multilayer construction," J. Alloys Compd., 808 (2019). doi:10.1016/j.jallcom.2019.07.342.
35) J. Yi, S. Chen, K. Chen, Y. Xu, Q. Chen, C. Zhu, and L. Liu, "Effects of ni content on microstructure, mechanical properties and inconel 718 cutting performance of altin-ni nanocomposite coatings," Ceram. Int., 45 (1) 474–480 (2019). doi:10.1016/j.ceramint.2018.09.192.
36) A. Shaikh, M. Yashin, A. Bogatov, M. Viljus, R. Traksmaa, J. Sondor, A. Lümkemann, F. Sergejev, and V. Podgurski, "High-temperature tribological performance of hard multilayer tin-altin/naco-crn/alcrn-alcroalticrn coating deposited on wc-co substrate," Coatings, 10 (9) (2020). doi:10.3390/COATINGS10090909.
37) S. Chowdhury, B. Bose, A.F.M. Arif, and S.C. Veldhuis, "Improving coated carbide tool life through wide peening cleaning (wpc) during the wet milling of h13 tool steel," Wear, 450–451 (2020). doi:10.1016/j.wear.2020.203259.
38) M. Szala, M. Walczak, K. Pasierbiewicz, and M. Kamiński, "Cavitation erosion and slidingwear mechanisms of altin and tialn films deposited on stainless steel substrate," Coatings, 9 (5) (2019). doi:10.3390/COATINGS9050340.
39) F. Cai, Y. Gao, W. Fang, T. Mao, S. Zhang, and Q. Wang, "Improved adhesion and cutting performance of altisin coatings by tuning substrate bias voltage combined with ar ion cleaning pre-treatment," Ceram. Int., 44 (15) 18894–18902 (2018). doi:10.1016/j.ceramint.2018.07.125.
40) K. Mughal, M.Q. Saleem, and M.P. Mughal, "Performance evaluation of nano-composite ceramic-coated high-speed steel (hss) drills in high-speed machining," Int. J. Adv. Manuf. Technol., 96 (9–12) 4195–4203 (2018). doi:10.1007/s00170-018-1829-9.
41) G. Singh, S. Singh, and J.S. Grewal, "Erosion wear characterisation of dlc and alcrn-based coated aisi-304/316 steels," Surf. Eng., 35 (4) 304–316 (2019). doi:10.1080/02670844.2018.1478685.
42) K. Aslantaş, H.E. Hopa, M. Percin, I. Ucun, and A. Çiçek, "Cutting performance of nano-crystalline diamond (ncd) coating in micro-milling of ti6al4v alloy," Precis. Eng., 45 55–66 (2016). doi:10.1016/j.precisioneng.2016.01.009.
43) T. Bakalová, N. Petkov, H. Bahchedzhiev, P. Kejzlar, and P. Zdobinská, "Tribological properties of tin/altin and altin/tin nanomultilayer coatings," Manuf. Technol., 16 (6) 6–7 (2016). doi:10.21062/ujep/x.2016/a/1213-2489/MT/16/6/1234.
44) K. Gangatharan, N. Selvakumar, P. Narayanasamy, and G. Bhavesh, "Mechanical analysis and high temperature wear behaviour of alcrn/dlc coated

titanium alloy," Int. J. Surf. Sci. Eng., 10 (1) 27–40 (2016). doi:10.1504/IJSURFSE.2016.075315.

45) S. Singh, R. Kumar, P. Goel, and H. Singh, "Analysis of wear and hardness during surface hardfacing of alloy steel by thermal spraying, electric arc and tig welding," Mater. Today Proc., 50 1599–1605 (2022). doi:10.1016/j.matpr.2021.09.122.
46) K. Badogu, V. Thakur, R. Kumar, R. Kumar, and S. Singh, "Acrylonitrile butadiene styrene-zro2 composites for roller burnishing as post-processing of 3d printed parts: machine learning modeling using classification and regression trees," J. Mater. Eng. Perform., 33 (18) 9522–9533 (2024). doi:10.1007/s11665-023-08620-y.
47) A.S. Channi, H.S. Bains, J.S. Grewal, V.S. Chidambranathan, and R. Kumar, "Investigation of tool wear rate during edm for aluminium metal matrix composite (5-10% tib2) prepared by squeeze casting," J. Electrochem. Sci. Eng., (2022). doi:10.5599/jese.1391.
48) N. Ranjan, R. Kumar, R. Kumar, R. Kaur, and S. Singh, "Investigation of fused filament fabrication-based manufacturing of abs-al composite structures: prediction by machine learning and optimization," J. Mater. Eng. Perform., 32 (10) 4555–4574 (2023). doi:10.1007/s11665-022-07431-x.
49) B. Erappa Rajj, M. Nagaral, S. Chintakindi, R. Kumar, A.E. Anqi, A.A. Rajhi, A.A. Duhduh, G. Sridevi, C. Prakash, R. Kumar, and C.K. Chan, "Nano-sized al 2 o 3 –gr reinforced al7075 hybrid composite: impact of cooling agents on mechanical, wear, and fracture behavior," ACS Omega, 9 (16) 17878–17890 (2024). doi:10.1021/acsomega.3c08822.
50) V. Thakur, R. Kumar, R. Kumar, R. Singh, and V. Kumar, "Hybrid additive manufacturing of highly sustainable polylactic acid -carbon fiber-polylactic acid sandwiched composite structures: optimization and machine learning," J. Thermoplast. Compos. Mater., 37 (2) 466–492 (2024). doi:10.1177/08927057231180186.
51) K. Singh, R. Kumar, S. Singh, R. Kumar, F.F. Sead, and J. Lozanović, "Non-conventional machining of monel-400 alloy: a critical review of techniques, challenges, and sustainable prospects," Front. Mech. Eng., 11 (2025). doi:10.3389/fmech.2025.1639320.
52) S. Singh, H.S. Farwaha, R. Kumar, I.A. Ariffin, N. Beemkumar, J.S. Grewal, I. Singh, A. Bhowmik, and W. Fendzi Mbasso, "Slurry erosion performance of wc-co and cr3c2-nicr coatings on hydro turbine steel: optimization and modelling under variable operational conditions," Oxford Open Mater. Sci., 5 (1) (2025). doi:10.1093/oxfmat/itaf008.
53) A. Aherwar, A. Ahirwar, and V.K. Kumar Pathak, "Dry sliding tribological characteristics evaluation and prediction of tib2-cda/al6061 hybrid composites exercising machine learning methods," Sci. Rep., 15 (1) (2025). doi:10.1038/s41598-025-01336-0.
54) P. Kumar, and B. Kumar, "Synergistic approach to tribological characterization of hybrid aluminum metal matrix composites with zrb2 and fly ash: experimental and predictive insights," Proc. Inst. Mech. Eng. Part E J. Process Mech. Eng., (2024). doi:10.1177/09544089241255931.
55) M. Kupczyk, M. Lelen, J. Józwik, and P. Tomiło, "Modeling material machining conditions with gear-shaper cutters with tin0.85-ti in adhesive wear dominance using machine learning methods," Materials (Basel)., 17 (22) (2024). doi:10.3390/ma17225567.
56) S. Sathiyamurthy, S. Sengottaiyan, and V. Vinoth, "Enhancing tribological performance of hybrid fiber-reinforced composites through machine learning and response surface methodology," J. Reinf. Plast. Compos., (2024). doi:10.1177/07316844241256421.
57) S. Sengottaiyan, S. Subbarayan, V. Vinoth, and P. Pugazhendi, "Optimized machine learning with hyperparameter tuning and response surface methodology for predicting tribological performance in bio-composite materials," Polym. Compos., 45 (10) 9421–9439 (2024). doi:10.1002/pc.28418.

Cite: A. Kaur, J. Dureja, J. Grewal, "Enhancing Wear Resistance of EN-19 Steel with Physical Vapor Deposition (PVD) Coatings: Experimental and Statistical Analysis". Evergreen, 13 (02) 517-536 (2026). https://doi.org/10.5109/7420066.